Planet. Space Sci. 1969, Vol. 17, pp. 321 to 331. Pergamon Press. Printed in Northern Ireland

# PRELIMINARY COMPARISON OF SOLAR WIND PLASMA OBSERVATIONS IN THE GEOMAGNETOSPHERIC WAKE AT 1000 AND 500 EARTH RADII

DEVRIE S. INTRILIGATOR*, JOHN H. WOLFE, DARRELL D. McKIBBIN and HAROLD R. COLLARD

Space Sciences Division, NASA-Ames Research Center, Moffett Field, Calif. 94035, U.S.A.

**Abstract**—Preliminary comparison of observations in the expected region of the geomagnetic tail with the Ames Research Center solar wind plasma probe at 1000 Earth radii (Pioneer 7, September 1966) and 500 Earth radii (Pioneer 8, January 1968) indicates that the measured plasma characteristics in these regions are similar. In each case intervals of quiescent plasma ion energy spectra are interrupted by abrupt changes in the magnitude and shape of the ion spectra or by complete absence of measurable plasma. Each of these regions is highly disturbed and is most appropriately described by the term 'geomagnetospheric wake'. A comparison with measurements in the near-Earth region of the geomagnetic tail indicates that the characteristics of the geomagnetic tail apparently undergo significant changes between $80R_E$ and $500R_E$.

## INTRODUCTION

There has been considerable interest in predicting and measuring the characteristics of the geomagnetic tail and the distance to which it extends (Dessler, 1964, 1968; Dungey, 1965; Piddington, 1960). There have been a number of spacecraft that have explored the tail in cislunar space. It has been found (Wolfe *et al.*, 1966a; Gringauz *et al.*, 1966; Ness *et al.*, 1965, 1967) that the geomagnetic tail at these near distances is well-ordered and well-defined. Mariner IV passed through the expected region of the geomagnetic tail at $3300R_E$ and found no evidence of the tail extending to this distance (Coleman *et al.*, 1965; Van Allen, 1965).

Pioneer 7, launched August 17, 1966, passed through the expected region of the geomagnetic tail at $1000R_E$ (Wolfe *et al.*, 1967; Ness *et al.*, 1967). Preliminary analysis of the data indicated that this region was quite disturbed and therefore unlike the geomagnetic tail in cislunar space. To indicate the nature of the measured plasma characteristics, Wolfe *et al.* denoted this as the region of the 'geomagnetospheric wake'.

Since that time Explorers 33 and 35 have extended the measurements of the near-Earth tail out to a distance of $80R_E$ and measurements show that the tail at these distances is still well-ordered and well-defined (Mihalov and Sonett, 1968; Behannon, 1968).

Pioneer 8, launched December 13, 1967, had a trajectory that was tailored so that the spacecraft would pass through the expected region of the geomagnetic tail at $500R_E$.

In this paper we will compare the plasma characteristics of the tail-associated phenomena measured by the Ames Research Center (ARC) solar wind plasma probe on Pioneer 8 with the plasma characteristics measured by the ARC solar wind plasma probe on Pioneer 7. Plasma ion data obtained with each instrument will be presented. The trajectories of the two spacecraft are shown in Fig. 1.

## INSTRUMENTATION

The ARC solar wind plasma probe on Pioneer 8 is basically similar to the ARC plasma probes on Pioneers 6 and 7 (Wolfe *et al.*, 1966b) in that it is also a multicollector electrostatic analyzer with truncated concentric hemispherical plates. Figure 2 illustrates the

* NRC-NAS Postdoctoral Resident Research Associate.

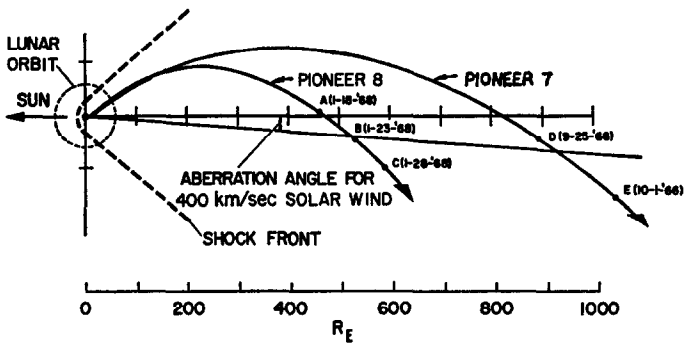


FIG. 1. PIONEERS 7 AND 8 TRAJECTORIES. ECLIPTIC PROJECTION.
Pioneer 7, launched August 17, 1966, went through the expected region of the geomagnetic tail at $1000R_E$ in September 1966. Pioneer 8, launched December 13, 1967, went through the expected region of the geomagnetic tail at $500R_E$ in January 1968. The Pioneer 8 spacecraft coordinates at locations *A*, *B* and *C* are, respectively, $460R_E$, $525R_E$ and $590R_E$ geocentric from the Earth; $8{\cdot}5R_E$, $10{\cdot}5R_E$ and $12{\cdot}3R_E$ above the ecliptic at an ecliptic projection of the Spacecraft–Earth–Sun angle of 180°, 185·5° and 190·5°. The Pioneer 7 spacecraft locations at *D* and *E* are, respectively, $887R_E$ and $1059R_E$ geocentric from the Earth, $25{\cdot}4R_E$ and $28{\cdot}7R_E$ above the ecliptic at an ecliptic projection of the Spacecraft–Earth–Sun angle of 183° and 189°.

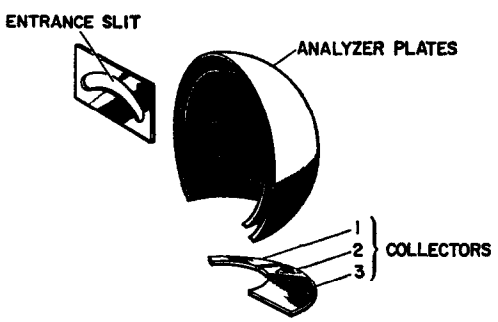


FIG. 2. EXPLODED VIEW OF THE AMES RESEARCH CENTER PLASMA PROBE FLOWN ON PIONEER 8.

detector indicating the 120° total parallel plate curvature and the three collectors. In order to provide a large dynamic range the collectors may be operated with or without the suppression of secondary electrons. Voltage applied across the analyzer plates deflects charged particles lying in the proper range of energy per unit charge ($E/Q$) values through the system to the three collectors. Ions are detected in 30 logarithmically spaced energy per unit charge steps from 150 to 15,000 V. There is an electron mode of operation (when the analyzer plate polarity is reversed) in which electrons are measured in 14 logarithmically spaced energy per unit charge steps ranging from 12 to 1000 V. There is also a zero energy per unit charge background step. In this paper only plasma ion measurements will be discussed. A complete ion energy (energy per unit charge) spectrum is measured approximately every 60 sec. The instrument is designed to make detailed angular measurements. The polar and azimuthal angular resolutions of the instrument are illustrated in Fig. 3. Azimuthal angles are measured in 23 sectors in the equatorial plane of the spacecraft. Seventeen sectors ($2\frac{1}{16}°$ wide) bracket the solar direction as determined by referencing the normal to the instrument aperture to the spacecraft Sun sensor pulse. Polar angles are

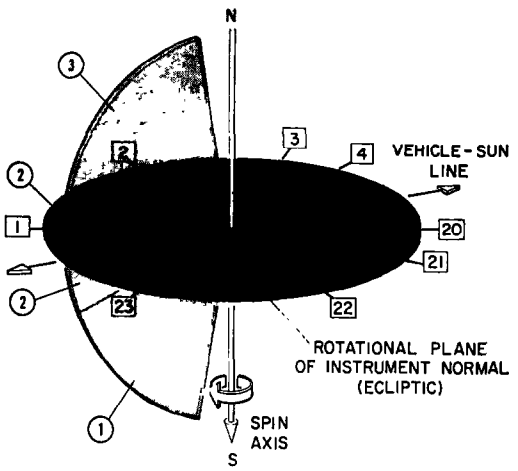


FIG. 3. PIONEER 8 AMES PLASMA PROBE ANGULAR VIEW.
The Ames instrument has both polar and azimuthal angular resolution. Numbers 1, 2 and 3 indicate the approximate polar acceptance of each of the three collectors. Collector 2 views the latitude angular band bracketing the ecliptic from approximately $-10°$ to $+10°$, collectors 1 and 3 from $-85°$ to $-10°$ and $+10°$ to $+85°$, respectively. For azimuthal resolution the spacecraft rotational plane (ecliptic) is segmented into 23 sectors as indicated. The 17 fine sectors (sectors 4 through 20) that bracket the solar direction are each 2 13/16° wide in ecliptic longitude. All other sectors have the same width but are more widely spaced. The spin axis of the spacecraft (and plasma probe) points toward the South ecliptic pole.

measured by comparing relative currents on the three collectors. Collector 2 brackets the ecliptic plane and measures particles incident from the neighborhood of this plane. Collector 1 measures ions incident from below this plane while collector 3 measures ions incident from above. Angular scans for all 30 energy steps are completed every 60 revolutions of the Pioneer 8 spacecraft, i.e., approximately every 60 sec.

## CALIBRATION

In order to predict accurately the instrument response to any arbitrary particle distribution, a detailed instrument calibration was performed. The collector amplifiers were first individually calibrated with a current source, and then the analyzer plate potentials for all the $E/Q$ steps were measured.

The instrument was mounted in a gimbal within a vacuum chamber. The calibration was performed with a mass analyzed $H^+$ beam which was flat over the instrument aperture to within $\pm 3$ per cent and time stable for the duration of calibration to within $\pm 5$ per cent. The distance from the ion source to the instrument was approximately 12 ft. This provided a laminar flow for the beam at the instrument aperture. The absolute beam flux was measured through the use of a geometrically suppressed Faraday cup as a primary standard and a gridded Faraday cup as a secondary standard. With a fixed beam energy, the angular acceptance of each collector was determined by rotating the gimbal and recording the instrument responses. Similarly, the energy acceptance was determined by varying the deflection potentials within the instrument. A comparison of the response of the instrument operated with the collectors in suppressed mode (suppression of secondary electrons) and unsuppressed mode was made. This comparison allowed the determination of the secondary electron coefficients, and with these coefficients the instrument response at all the other ion energy ($E/Q$) steps.

The calibration results have been utilized in the reduction of the plasma data presented here.

## ION ENERGY SPECTRA

As a means of examining the plasma ion energy distribution and determining whether its characteristics are steady or fluctuating we plot ion energy spectra. These are smoothed contour plots of the peak cold beam equivalent (CBE) flux in each energy per unit charge ($E/Q$) step versus the voltage range of the $E/Q$ step. A 'typical' interplanetary solar wind ion energy spectrum is shown in Fig. 4a. The peak of the curve (the $H^+$ peak) is $10^7$–$10^8$ ions

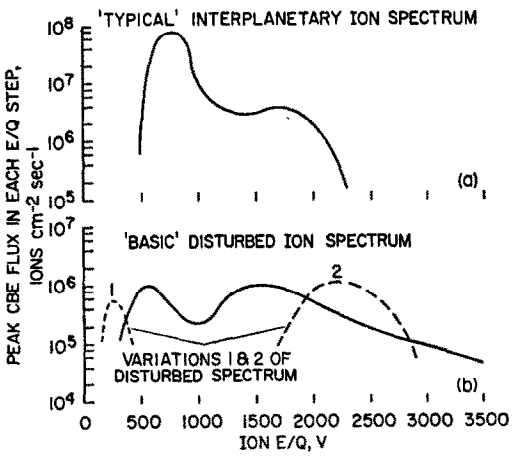


FIG. 4. PIONEER 7 ION SPECTRUM.
(a) 'Typical' interplanetary ion spectrum (see text). The peak CBE flux of the curve (the $H^+$ peak) is $10^7$–$10^8$ ions $cm^{-2}$ $sec^{-1}$. The energy per unit charge is 850 V. The second peak at 1700 V (2 × 850 V) is the $He^{++}$ peak. (b). 'Basic' disturbed ion spectrum and two variations often observed in the geomagnetospheric wake. The peak flux is $<\sim 10^6$ ions $cm^{-2}$ $sec^{-1}$. In this case the first peak of the curve (the $H^+$ peak) occurs at ~500 V and the second at ~1500V. The second peak is interpreted as a high energy tail of the proton energy distribution. Analysis of successive ion spectra show that the higher energy distribution often grows at the expense of the lower energy distribution. At times only part of the distribution is seen as indicated by the two variations.

$cm^{-2}$ $sec^{-1}$ and the energy per unit charge of this peak is 850 V. There is a second peak at 1700 V (2 × 850 V) which is identified as the $He^{++}$ peak. Analysis of Pioneer 7 data shows that in the region of the geomagnetospheric wake the 'typical' ion energy spectrum is often not observed. The 'basic' disturbed ion energy spectrum and two variations of this spectrum that are observed are shown in Fig. 4b. The peak of the curve of the disturbed ion energy spectrum is usually one to two orders of magnitude less than that of the 'typical' interplanetary ion energy spectrum. The disturbed ion energy spectrum is often characterized by a different type of double peak, and analysis of successive spectra show that the higher energy peak (the high energy tail of the proton energy distribution) often grows at the expense of the lower energy distribution.

Two series of Pioneer 7 ion spectra from September 30, 1966 are shown in Fig. 5. Both series of spectra were measured within a few minutes of each other. The first series is similar to the typical interplanetary ion spectra, the second, to the disturbed. With the exception of the last two spectra (17H 37M 43S and 17H 38M 33S) the measured successive ion spectra shown in Fig. 5 are quite similar and therefore indicative of the true ion energy distribution. However, there are frequently intervals in this extended tail region as observed

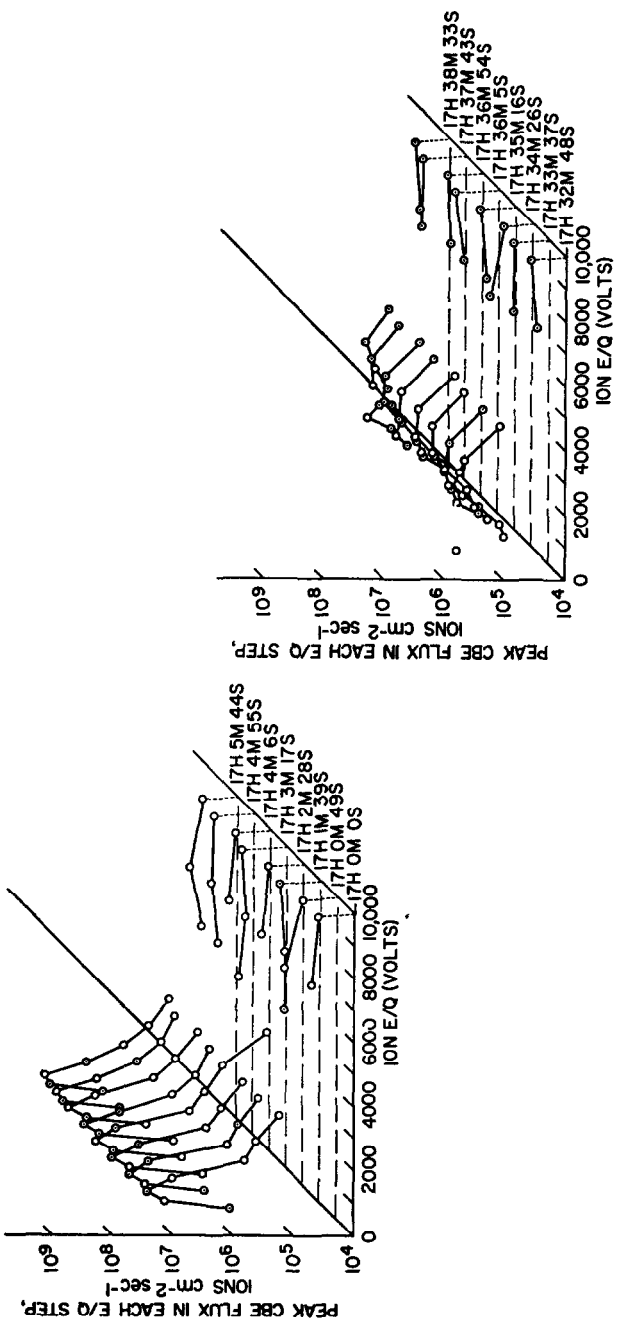


FIG. 5. PIONEER 7 ION SPECTRA. SEPTEMBER 30, 1966.
The series on the left (17H 00M 00S to 17H 05M 44S) are similar to the typical interplanetary ion spectrum (Fig. 4a). The series on the right (17H 32M 48S to 17H 38M 33S) is an example of a disturbed series of spectra seen in the geomagnetospheric wake. The peak intensities of the disturbed spectra are one to two orders of magnitude less than those of the more typical spectra. The general shapes of the two types of spectra are different and the location of the peak of the curve is at a higher $E/Q$ step in the disturbed spectra indicating the growth of the high energy tail of the proton energy distribution.

on Pioneers 7 and 8 when the ion energy distribution is so rapidly changing that the measured ion energy spectra are time aliased. Figure 6 shows two series of ion spectra. The series on the left shows one spectrum for each of the 24 hr as measured on Pioneer 8 on January 23, 1968. The series on the right shows each individual spectrum for the interval from 0830 to 1030 UT on January 23, 1968. In general the spectra are 'ragged' and time aliased, indicating that the measurable plasma characteristics are rapidly changing. The figure illustrates that there are some intervals (e.g. 0910–0915 UT) when there is an absence of measurable plasma within the energy range of the detector and others (e.g. 0830–0845 UT) where the observed plasma has a relatively high energy distribution peaking between 3 and 4 kV.

## PIONEER ION DATA

For routine reduction of our interplanetary solar wind data a computer program has been designed that assumes that a Maxwell–Boltzmann distribution adequately describes the proton temperature distribution in the ion energy spectra, and from this various plasma parameters such as proton number density, velocity and temperature are computed. From the angular data the polar angle of flow and azimuthal angle of flow are determined. However, at times when the measured plasma characteristics are rapidly changing the ion energy spectra and the angular sweeps are often aliased and the rote computation to determine the plasma parameters is unreliable. In an attempt to summarize the data from successive ion spectra and angular sweeps when the distributions are rapidly changing we have developed programs that compute the peak CBE flux in the peak $E/Q$ step (ions $cm^{-2}$ $sec^{-1}$), the velocity of the peak flux (km $sec^{-1}$) and the azimuthal angle associated with the peak flux (deg). The peak flux is determined by looking at the azimuthal angle scans (azimuthal sweeps) at all $E/Q$ steps and selecting the highest of the peak CBE fluxes measured and then fitting a parabola to the three points determined by that flux reading and the adjacent flux readings. From the peak of the parabola the value of the peak flux and the azimuth of the peak flux are determined. The velocity of the peak flux is determined similarly from fitting a parabola to the peak CBE flux (in each $E/Q$ step) reading vs. $E/Q$ for the energy step at which the peak flux was observed and the two adjacent energy steps. The peak flux velocity is then calculated from the value of $E/Q$ corresponding to the peak of the parabola.

In Fig. 7 there are plots of the peak CBE flux in the peak $E/Q$ step and the velocity and angle of flow associated with it. These data are from the same time interval (0830–1030 UT) as the detailed ion spectra shown in Fig. 6. No data are plotted in this figure from before 0830 UT or after 1030 UT . From 0830 to 0914 the peak flux is always less than $10^5$ ions $cm^{-2}$ $sec^{-1}$. There is no measurable flux from 0847 to 0857 and from 0909 to 0914. When there is a measurable ion distribution the measured velocity of the peak flux is unusually high (greater than 800 km $sec^{-1}$). The ion energy spectra in Fig. 6 also indicate that when there is a measurable ion distribution during this interval it is characterized by an enhancement of the high energy tail of the proton distribution. These low flux, high velocity measurements imply an extremely low ion density ($\ll 1$ ion $cm^{-3}$). Referring again to Fig. 7, there is an extended interval (0914–1028) of low peak flux (2–4 $\times$ $10^5$ ions $cm^{-2}$ $sec^{-1}$) and a lower velocity (300–400 km $sec^{-1}$) associated with that peak. By looking again at the ion spectra in Fig. 6, it can be seen that the high energy tail of the proton distribution is in general no longer present and instead the lower energy proton distribution is gradually growing. From 0915 to 0952 the spectra are time aliased and indicate that the distribution is in a state of change. From 0953 to 1016 the successive spectra are more similar and

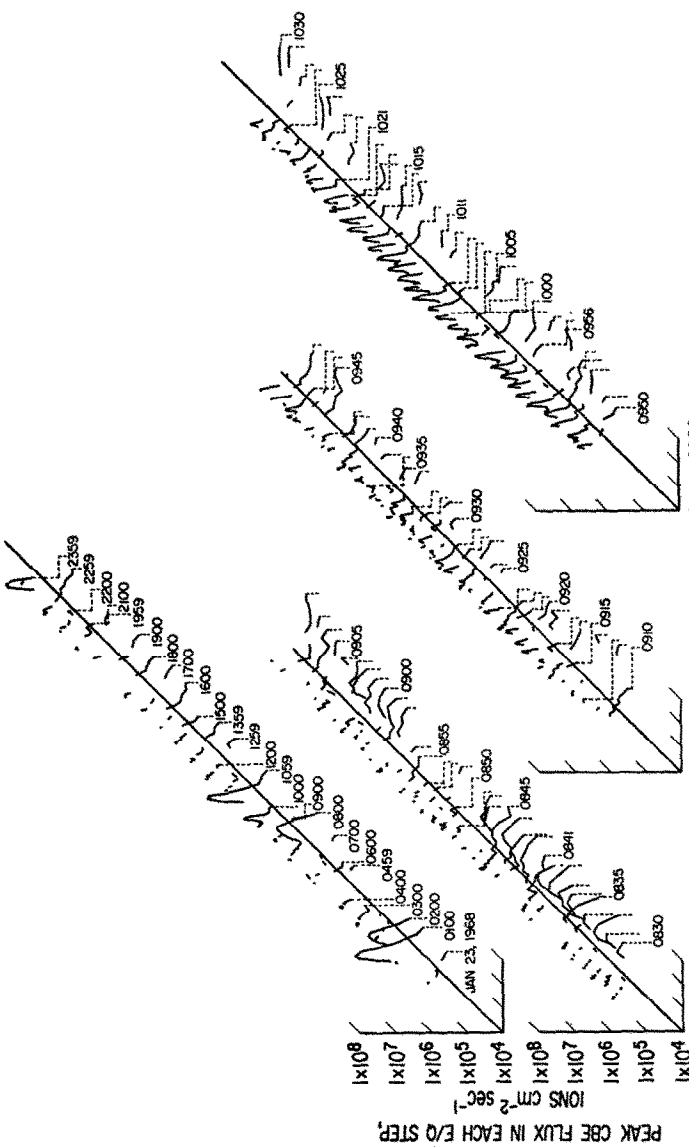


FIG. 6. ION SPECTRA IN THE GEOMAGNETOSPHERIC WAKE. PIONEER 8, JANUARY 23, 1968.
The series of 24 spectra on the left are the hourly spectra from 0000 to 2400 UT. Detailed spectra for the interval from 0830 to 1030 UT are shown in the series on the right. The spectra are often time aliased and 'ragged' indicating that the ion $E/Q$ distribution is rapidly changing. The dashed lines extend across to indicate the time of the measurement.

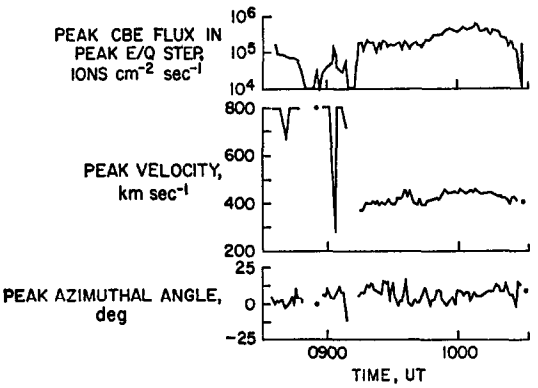


FIG. 7. PLASMA ION CHARACTERISTICS. PIONEER 8, JANUARY 23, 1968.
Data only from 0830 to 1030 UT are plotted. The three plots summarize (see text) the detailed ion spectra shown in Fig. 6. Intervals of low peak flux ($<10^6$ ions cm$^{-2}$ sec$^{-1}$) and high peak velocity ($>600$ km sec$^{-1}$) imply extremely low ion densities ($\ll 1$ ion cm$^{-3}$).

indicate that the plasma distribution is no longer changing as rapidly. After 1017 the ion distribution is aliased and changing again.

Pioneer 8 data from 1156 to 1700 UT on January 18, 1968 are shown in Fig. 8. Figure 8 is similar to Fig. 7, showing the peak flux, the peak velocity and the angle of flow associated with the peak flux. In addition, Fig. 8 also indicates the broadband wave level obtained from the TRW Systems VLF Electric Field Detector on Pioneer 8 (Scarf *et al.*, 1968). The threshold of this detector is at 5·5 mV. In general, it has been found that there is a good correlation between low amplitude (or threshold readings) of the broadband wave levels (Scarf, private communication) and low ion flux (or absence of measurable ion flux) of the plasma probe. The successive ion energy spectra associated with part of this time interval are shown in Fig. 9. It can be seen that before the interval of almost complete absence of

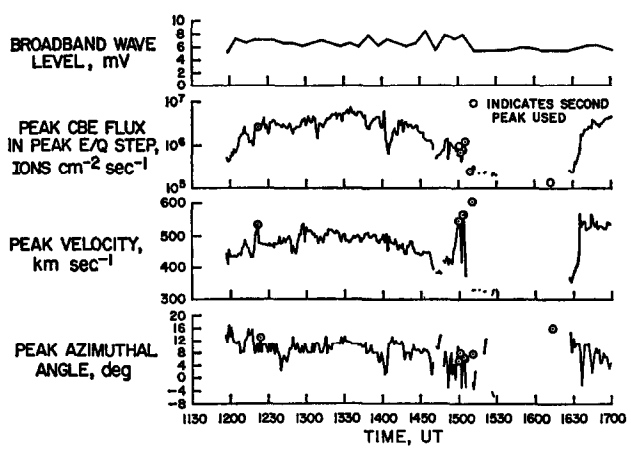


FIG. 8. PIONEER 8 DATA FROM 1156 to 1700 UT ON JANUARY 18, 1968.
This figure is similar to Fig. 7. In addition to the plasma parameters the broadband wave level obtained from the TRW Systems VLF Electric Field Detector on Pioneer 8 (Scarf *et al.*, 1968) is also shown. Note the absence of measurable plasma from 1515 to 1630 UT (see also Fig. 9) and the simultaneous drop in the amplitude of the broadband wave level to threshold (5·5 mV). When the second peak is used the velocity is computed for protons.

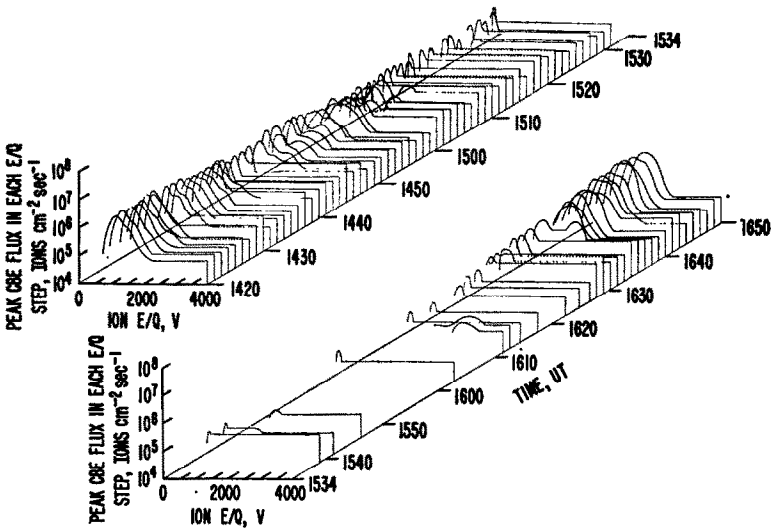


FIG. 9. PIONEER 8 ION SPECTRA, JANUARY 18, 1968.
This shows detailed spectra for an interval (1420–1650 UT) of data for which the plasma parameters are summarized in Fig. 8. In each curve a line is extended from the last data point shown across to the right and then down to indicate the time of the measurement. There is an interval (1531–1630 UT) of almost a complete absence of measurable plasma. Both immediately before and after this interval the spectra are disturbed and often aliased.

measurable plasma (~1531 UT) the spectra are disturbed. Between ~1452 and 1500 UT, for example, the ion energy distribution is changing and the high energy tail of the proton distribution is growing. Between 1500 and 1510 the spectra are even more time aliased and the proton distribution at higher energies is still growing. From 1510 to approximately 1531 the spectra are also aliased, but there is no longer a measurable high energy tail. For approximately the next hour (~1531–1630) there is almost a complete absence of measurable plasma. Between 1630 and 1640 the ion spectra begin reappearing, and between 1640 and 1650 the measurable intensities increase.

In Fig. 10 some ion energy spectra from Pioneer 8 from January 18, 1968 through January 28, 1968 are presented. For these eleven days spectra approximately 2 hr apart are plotted. This figure illustrates the changing nature of the measurable plasma characteristics during eleven of the days when the Pioneer 8 spacecraft was in the expected region of the geomagnetic tail at a downstream distance of approximately $500R_E$. Since these measurements were performed so recently the data from all the tracking stations are not as yet available. Therefore, to obtain Fig. 10 the real time teletype data were analyzed. However, there are some intervals when there are no teletype data. It is necessary to distinguish these data gaps (of greater than 2 hr) from intervals where there are data, but during which no measurable plasma is observed. In Fig. 10 an absence of measurable plasma is indicated by a low-lying noise spectrum (e.g. 1200–1800 UT on January 23, 1968) while a data gap is indicated by not plotting any spectrum at all (e.g. 2000–2400 UT on January 23, 1968).

## DISCUSSION

Pioneer 8 passed through the expected region of the geomagnetic tail in January 1968. Figures 6 through 10 present examples of some of the ARC solar wind plasma probe ion

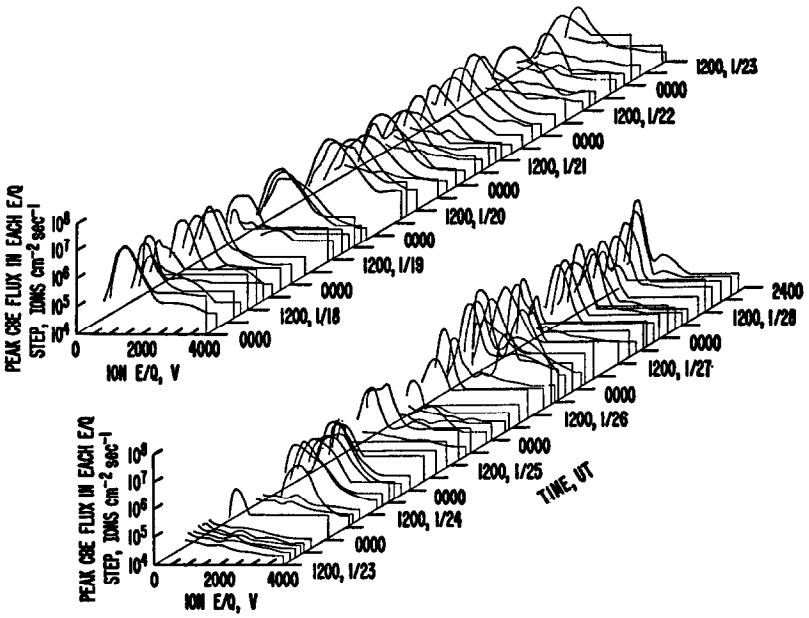


FIG. 10. PIONEER 8 ION SPECTRA, JANUARY 18–28, 1968.
Eleven days of spectra (approximately 2 hr apart) are plotted. The changing nature of the measurable plasma characteristics are illustrated. Real time teletype data gaps are indicated by not plotting any spectrum (e.g. 2000–2400 UT on January 23, 1968), while an absence of measurable plasma is indicated by plotting a low-lying noise spectrum (e.g. 1200–1800 on January 23, 1968). See Fig. 9 for explanation of horizontal lines.

data obtained on Pioneer 8 in January, 1968. Even though there were some changes in geomagnetic activity recorded at ground stations during this month, we interpret the data presented in these five figures as being examples of the apparent encounter of geomagnetic tail associated phenomena by the Pioneer 8 spacecraft at 500 Earth radii during this time period. In addition the ion spectra shown in Figs. 6, 9 and 10 are remarkably similar to those obtained during the Pioneer 7 encounter with the geomagnetospheric wake at 1000 Earth radii in September 1966. Therefore, the data presented here seem to imply that the term 'geomagnetospheric wake' that was used by Wolfe *et al.* (1967) to denote the plasma characteristics observed on Pioneer 7 at $1000R_E$ is also an applicable description of the observed region at $500R_E$.

The intermittent nature of the encounters of the geomagnetospheric wake by the spacecraft is also illustrated in Figs. 6 through 10. The data in Figs. 6 and 7, for example, show that the plasma probe measured an absence of flux from 0545 to 0720 UT and from ~0830 to 0845 UT. Whether the intervals of plasma observed from 0745 to 0830 and from 0850 to 0930 indicate the spacecraft was out of the wake region or whether they indicate that it was just within another plasma segment, also associated with the wake, will have to await a more detailed analysis.

Figures 4b, 5, 6, 9 and 10 show, however, that when there is a measurable plasma flux the shape of the ion spectra are often different from those associated with the typical interplanetary spectrum (Fig. 4a). In addition, the ion energy distribution is often changing so rapidly that the ion spectra are time aliased. Whether there is a need for a distinction between intervals during which these two types of non-'typical' interplanetary spectra (Fig. 4b) are measured and intervals during which there is a complete absence of measurable

plasma (possibly a result of the detection threshold of the instrument) must also await further study.

Both the disturbed nature of the measurable plasma characteristics and the intermittent intervals over which they are observed apparently indicate that even in the expected region of the geomagnetic tail at 500 Earth radii these measured plasma characteristics are very different from those associated with the tail within 80 Earth radii. The characteristics of the geomagnetic tail therefore appear to undergo significant changes between 80 and 500 Earth radii. Further analysis of the plasma ion and electron characteristics and comparisons with simultaneous electric and magnetic field measurements are needed to better define the characteristics and extent of the geomagnetic tail.

At this time it is not possible to distinguish between several possibilities:

(1) If the Earth's magnetosphere has closed between 80 and 500 Earth radii, then the observations could be those of the turbulent downstream wake.

(2) If the solar wind has diffused into the geomagnetic tail, then the observations could be those of the tail flapping past the spacecraft.

(3) If, at these extended distances, the tail has a filamentary structure, possibly quite intertwined, then the observations could be those of the various filaments.

(4) If the tail has broken up into 'bundles' which are not connected to the Earth, then the observations could be those of some of the bundles travelling past the spacecraft.

(5) If magnetic merging (Dungey, 1965) has taken place, then the observations could be those of the subsequent acceleration of pinched-off gas to near solar wind velocities.

It is anticipated that further analysis may shed light on the actual physical processes taking place at these distances.

*Acknowledgements*—The authors are grateful to Dr. F. L. Scarf of TRW Systems for generously providing broadband data from the Pioneer 8 VLF Electric Field Experiment and to the Ames Research Center Pioneer Project personnel under the direction of Mr. C. F. Hall for their untiring efforts in insuring the success of the Pioneer missions. Mr. R. H. Mason of the Pioneer Project deserves special credit for the tech nical management of the experiment. Thanks are given to Mr. A. S. Natwick for his assistance in obtaining data from the Pioneer missions.

## REFERENCES

BEHANNON, KENNETH W. (1968). Mapping of the Earth's bow shock and magnetic tail by Explorer 33. *J. geophys. Res.* **73**, 907–930.

COLEMAN, P. J., JR., L. DAVIS, JR., D. E. JONES and E. J. SMITH (1965). Mariner 4 magnetometer observations (title only). *Trans. Am. geophys. Un.* **46**, 113.

DESSLER, A. J. (1964). Magnetic merging in the magnetospheric tail. *J. geophys. Res.* **69**, 3913–3918.

DUNGEY, J. W. (1965). The length of the magnetospheric tail. *J. geophys. Res.* **70**, 1753.

GRINGAUZ, K. I., V. V. BEZRUKIKH, M. Z. KHOKHLOV, L. S. MUSATOV and A. R. REMINZOV (1966). Signs of crossing by the Moon of the Earth's magnetosphere tail according to data of charged particle traps on the first artificial satellite of the Moon. *Dokl. Akad. Nauk. SSSR Geofiz.* **170**, 570–573.

MIHALOV, J. D. and C. P. SONETT (1968). The cislunar geomagnetic tail gradient in 1967. *J. geophys. Res.* **73**, 6837–6841.

NESS, N. F. (1965). The Earth's magnetic tail. *J. geophys. Res.* **70**, 2989–3005.

NESS, N. F., C. S. SCEARCE and S. CANTARANO (1967). Probable observation of the geomagnetic tail at $6 \times 10^6$ km by Pioneer 7. *J. geophys. Res.* **72**, 3769–3776.

PIDDINGTON, J. H. (1960). Geomagnetic storm theory. *J. geophys. Res.* **65**, 93–105.

SCARF, F. L., G. M. CROOK, I. M. GREEN and P. F. VIROBIK (1968). Initial results of the Pioneer 8 VLF electric field experiment. *J. geophys. Res.* **73**, 6665–6686.

VAN ALLEN, J. A. (1965). Absence of 40-keV electrons in the Earth's magnetospheric tail at 3300 Earth radii. *J. geophys. Res.* **70**, 4731–4739.

WOLFE, J. H., R. W. SILVA and M. A. MYERS (1966a). Observations of the solar wind during the flight of Imp 1. *J. geophys. Res.* **71**, 1319–1340.

WOLFE, J. H., R. W. SILVA, D. D. MCKIBBIN and R. H. MASON (1966b). The compositional, anisotropic and nonradial flow characteristics of the solar wind. *J. geophys. Res.* **71**, 3329–3335.

WOLFE, J. H., R. W. SILVA, D. D. MCKIBBIN and R. H. MASON (1967). Preliminary observations of a geomagnetic wake at 1000 Earth radii. *J. geophys. Res.* **72**, 4577–4581.